Available online at www.sciencedirect.com
ScienceDirect
Journal of Catalysis 254 (2008) 180–189
JOURNAL OF CATALYSIS
www.elsevier.com/locate/jcat

Effect of aluminium distribution in the framework of ZSM-5 on hydrocarbon transformation. Cracking of 1-butene

P. Sazama [a], J. Dědeček [a], V. Gábová [a], B. Wichterlová [a,*], G. Spoto [b], S. Bordiga [b]

[a] *J. Heyrovský Institute of Physical Chemistry of the Academy of Sciences of the Czech Republic, v. v. i., Dolejškova 3, CZ-182 23 Prague 8, Czech Republic*
[b] *Dipartimento Chimica IFM – NIS Centre of Excellence, Università di Torino, via P. Giuria 7, I-10125 Torino, and INSTM, Research Unit of Torino, Italy*

Received 30 July 2007; revised 7 December 2007; accepted 16 December 2007

Available online 22 January 2008

Abstract

The effect of the distribution of Al atoms in the framework of H-ZSM-5, controlled by zeolite synthesis, on the product yields in 1-butene conversion to low olefins, aromatics and paraffins has been investigated for a series of zeolites, both synthesized and commercial, with Si/Al ranging from 12.6 to 43.6. The ^{27}Al and ^{29}Si MAS NMR of the corresponding Na-ZSM-5 and their exchange capacities for Co(II) ions and quantitative analysis of d–d transitions of bare Co(II) ions in the dehydrated CoNa-ZSM-5 were used for determination of the population of the [Al–O–(Si–O)$_n$–Al] sequences in the framework. The Si–Al sequences with $n = 1$ were not present in the synthesized or commercial samples. The exchange capacity of Co(II) ions corresponded to the concentration of "close" framework Al atoms present mostly in the six-membered framework rings ($n = 2$) of the cationic sites. The concentration of "single" Al atoms was calculated from the difference between the total concentration of Al and twice the concentration of the exchanged Co(II) ions. The enhanced formation of aromatics in 1-butene conversion for H-ZSM-5 with similar Si/Al ratio, but higher concentration of "close" Al atoms in the framework is accounted for enhancing the rate of hydrogen transfer reactions, in contrast to samples with higher concentration of "single" Al atoms, where olefin cracking is preferred. As low-temperature (20 K) IR analysis of adsorbed hydrogen showed that the acid strength of the protonic sites in the H-ZSM-5 samples is very similar, the differences in the selectivity of 1-butene cracking and aromatization are thought to be caused by different distribution of framework Al atoms and thus also of the protonic sites. This finding opens a new potential for advanced tailoring of zeolite catalyst selectivity.

Keywords: H-ZSM-5; Al distribution; Catalytic cracking; Zeolite acidity; IR spectra H_2; Cracking of olefins

1. Introduction

Since the discovery of H-ZSM-5 zeolites [1], the structures and acid strengths of their strongly acidic bridging Si–OH–Al groups and electron acceptor Al-related sites, as potential active sites, have been a focus of attention. The linear relationship obtained between the concentrations of the bridging OH groups and the activities of H-ZSM-5 zeolites in acid-catalyzed transformations of hydrocarbons, like cracking of paraffins, alkylation of aromatics etc., indicated that the strength of these Brønsted sites is equal, at least with respect to the reactions of hydrocarbons [2]. There is also so far no evidence that the acid strengths of the OH groups are different in ZSM-5. Analysis of the H–H or C≡O vibrations of adsorbed hydrogen and carbon monoxide, respectively, as well as the corresponding shifts in the OH vibrations, indicated equal strength of the protonic sites of H-ZSM-5. Nevertheless, the IR spectra in the region of the OH and OD vibrations at low temperatures (120 K) exhibited, in addition to the dominant band around 3619 and 2670 cm^{-1}, respectively, additional bands indicating presence of various types of OH groups with respect to their structure [3].

Understandably, the location of the aluminium atoms in the zeolite frameworks controls the location of the strongly acidic protons countering the negative charge of the framework in the H-forms of zeolites. It is also well known that both the dimension and architecture of the pores where the protons are located affect the product composition in the acid-catalyzed reactions of paraffins and olefins via the shape-selective effect, which has been manifested predominantly for medium-pore zeolites

* Corresponding author.
E-mail address: wichterl@jh-inst.cas.cz (B. Wichterlová).

0021-9517/$ – see front matter
doi:10.1016/j.jcat.2007.12.005

with ZSM-5, ferrierite and mordenite structures [4–7]. However, in addition to the location of protons in the individual pores of these high-silica zeolites, the distances between the protons might be also expected to affect their function and reaction pathway in acid-catalyzed reactions. But the effect of aluminium distribution in the framework of high-silica zeolites on their activity, even for the most frequently employed ZSM-5 structure, has not been analyzed yet, because of lack of knowledge of the Al distribution in these zeolites.

The recent findings that (i) the distribution of Al in the framework of ZSM-5 zeolites is not random and is not controlled by statistical rules, (ii) the local Al distribution can be estimated from the distribution of the counter divalent cations (e.g., Co(II) ions) supplemented by ^{27}Al and ^{29}Si NMR investigations, see Refs. [8,9], and that (iii) in ZSM-5 zeolites, the Al distribution can be varied by the conditions of the zeolite synthesis [10] have led to studies of the effect of distribution of Al, and thus of acidic protons, on the catalytic reactions over H-ZSM-5 zeolites.

The variability of aluminium location in ZSM-5 zeolites comes from the high number of positions of T atoms in the framework of ZSM-5. The resolution of aluminium atoms at the individual T sites by ^{27}Al MAS NMR spectroscopy is practically impossible, as they exhibit close chemical shifts [11,12]. Nevertheless, recent combination of ^{27}Al 3Q MAS NMR spectroscopy and quantum chemical calculations of chemical shifts for a series of H-ZSM-5 samples with very low Al content has led to some progress in the identification of the individual T sites in the ZSM-5 framework [13].

^{29}Si MAS NMR provides information on the local environment of Si with respect to neighbouring Al [14]. In most samples of ZSM-5 zeolites employed, both commercial and synthesized in laboratories, two Al atoms neighbouring Si, Si (2Si2Al)—the [Al–O–Si–O–Al] sequences—do not occur. Large numbers of Si atoms are surrounded by four Si atoms, Si(4Si) or by one Al atom and three Si atoms, Si (3Si1Al). The latter surrounding occurs in [Al–O–(Si–O)$_n$–Al] sequences with both $n = 2$ and $n > 2$. Therefore, ^{29}Si MAS NMR cannot distinguish these sequences exhibiting relatively close Al atoms ($n = 2$) and very distant Al atoms ($n > 2$). Nevertheless, it has recently been shown [8,9] that the occurrence of the individual [Al–O–(Si–O)$_n$–Al] sequences in the framework can be estimated indirectly on the basis of the ion exchange capacity of the counter divalent Co(II) ions (not bearing negatively charged ligands) requiring two framework Al atoms in the vicinity to balance their charges [9]. It has been found that most of the exchanged [Co(H$_2$O)$_6$](II) complexes (>97%) in hydrated Co-ZSM-5 zeolites are balanced by the [Al–O–(Si–O)$_2$–Al] sequences located in the framework rings forming the cationic sites. Under zeolite dehydration, these Co complexes are transformed into bare Co(II) cations coordinated exclusively to the framework oxygens of the cationic sites. In dehydrated zeolites, the [Co(H$_2$O)$_6$](II) complexes, charge-balanced by two Al atoms belonging to different framework rings, form Co–oxo cationic species coordinated to extra-framework oxygen atom(s) in addition to the framework oxygen atoms, or they are transformed into Co oxide-like species. The population of the individual [Al–O–(Si–O)$_n$–Al] sequences can be obtained from the quantitative analysis of the UV–vis spectra of Co(II) ions and the value of the maximum Co(II) ion exchange capacity (for details see Refs. [8,9]). Therefore, this approach allows us to distinguish among three types of [Al–O–(Si–O)$_n$–Al] sequences:

(i) close Al atoms [Al–O–(Si–O)$_2$–Al], in which two aluminium atoms are located in one six-membered ring bridged by two Si atoms in the cationic sites. Local negative framework charge originating from the aluminium atoms in these "Al pairs" can be compensated by a bare divalent cobalt cation in dehydrated Co(II)-exchanged zeolites. The concentrations of the bare Co(II) ions (in the α-, β- and γ-type cationic sites; description of the sites see Ref. [15]), calculated from the intensities of the d–d bands of the vis spectra, are proportional to the concentrations of close Al atoms in one six-membered ring of the framework of ZSM-5 zeolites [9];
(ii) close Al atoms located in different framework rings. These two aluminium atoms are separated by two or more silicon-oxygen groups [Al–O–(Si–O)$_{n\geqslant 2}$–Al], but they are close enough to be balanced (in the hydrated as-prepared zeolites) by hexaaquocomplexes of the Co(II) cations. The concentration of this type of Si–Al sequences in the framework of ZSM-5 zeolites represents a difference between the value of the Co(II) ion-exchange capacity (obtained from chemical analysis) and the concentration of the bare divalent cobalt cations in dehydrated zeolites (obtained from quantitative analysis of the d–d vis spectra); and
(iii) single Al atoms in the [Al–O–(Si–O)$_{n>2}$–Al] sequences with only one Al atom in the six- or five-membered ring. This type of sequence is able to balance the charge of only a monovalent Co complex, but not a divalent Co(II) cation.

It can be considered that both types of close Al atoms (located in one or two framework six-membered rings) can bring about close protonic sites, in contrast to single Al atoms. Our previous results showed a significant influence of aluminium and silicon sources used for the synthesis of ZSM-5, on the distribution of Al in the framework of ZSM-5 zeolites [10]. Thus, this opened a possibility to study the effect of the aluminium distribution on the catalytic properties of the zeolites.

We selected cracking of 1-butene to ethene and propene, accompanied by the formation of C_5 olefins, aromatics and paraffins, to investigate the effect of the Si–Al sequences on the activity of H-ZSM-5 zeolites. Transformations of olefins, including double bond shift, skeletal isomerization and cracking proceed via a monomolecular mechanism, while a bimolecular mechanism is involved in dimerization and hydrogen-transfer reactions leading to aromatics and paraffins. Carbenium ions take part in both principal reaction pathways, monomolecular and bimolecular. The mechanisms including formation of carbenium cations, their isomerization and β-scission were described in detail in Refs. [16–18]. It was also shown that the preference for a mono- or bimolecular mechanism strongly de-

Table 1
Characteristics of ZSM-5 catalysts

Sample	Si/Al[a]	Si/Al[b]	Crystal size (μm)	Total Al[a] (mmol/g)	Single Al[c]		Close Al					
							Overall[c]		In one ring[d]		In different rings[d]	
					mmol/g	%	mmol/g	%	mmol/g	%	mmol/g	%
#1[e]	15.8	17	0.5	0.97	0.66	68	0.31	32	–	–	–	–
#2[e]	43.6	50	0.7	0.37	0.32	85	0.06	15	–	–	–	–
#3[e]	73.0	n.d.	3	0.22	–	–	–	–	–	–	–	–
#4[e]	149	n.d.	2.5	0.11	–	–	–	–	–	–	–	–
#5[e]	300	n.d.	3	0.06	–	–	–	–	–	–	–	–
#6[f]	12.6	12.5	5	1.20	1.01	84	0.19	16	–	–	–	–
#7[f]	26.8	25	0.3	0.59	0.38	64	0.21	36	0.193	33	0.018	3
#8[f]	28.6	30	0.5	0.56	0.52	93	0.04	7	–	–	–	–
#9[f]	37.4	35	0.6	0.43	0.39	90	0.04	10	–	–	–	–
#10[f]	37.9	n.d.	0.3	0.43	0.24	56	0.19	44	0.186	43	0.004	1
#11[f]	43.3	n.d.	0.3	0.37	0.22	58	0.16	42	0.141	37	0.019	5

[a] From chemical analysis of Na-ZSM-5.
[b] From ^{29}Si MAS NMR of Na-ZSM-5.
[c] From chemical analysis of Co(II) ions in Co-ZSM-5.
[d] From UV–vis spectra of dehydrated Co-ZSM-5.
[e] Commercial ZSM-5.
[f] ZSM-5 synthesized in the laboratory.

pends on the reaction conditions and the reactivity of the individual olefins and carbenium ions formed.

It should also be pointed out that the transformations of olefins have a major impact on the product composition in many processes, like conversion of methanol to gasoline, methanol to olefins, FCC of paraffins, alkylation of aromatics. Moreover, cracking of $C_4^=$–$C_6^=$ olefins itself has recently appeared to be a promising technology for production of propene and ethene, which are highly in demand as a major feedstock in polymer production [19–24].

As the overall concentration of acid sites and the crystal size of zeolites are known to substantially affect the product composition in acid-catalyzed transformation of hydrocarbons, the effect of the population of close Al atoms and single Al atoms in the zeolite framework on the zeolite activity was investigated on samples exhibiting close values of these parameters. Furthermore, both the local density of protonic sites and their acid strength can be expected to contribute to cracking, oligomerization and aromatization of olefins. Therefore, the acid strength of the protonic sites of the samples has been analyzed by hydrogen adsorption at low temperatures. The position of the H–H vibration and the related shift of the OH vibration were used as a measure of the acid strength. The relative concentration of close Al atoms was determined from the Co(II) ion-exchange capacity and supported by the UV–vis spectra (d–d and charge-transfer transitions) of the Co(II) ions in the dehydrated zeolites.

2. Experimental

2.1. Preparation of ZSM-5 zeolites

Table 1 lists ZSM-5 zeolites used in this study. ZSM-5 zeolites with Si/Al 15.8, 43.6, 73.0, 149 and 300 were purchased from Conteca, and ZSM-5 zeolites with Si/Al 12.6, 26.8, 28.6, 37.4, 37.9, 43.3 were synthesized in our laboratory by using various sources of aluminium and synthesis conditions to obtain samples with different distribution of aluminium in the framework.

Table 2
Synthesis of ZSM-5 zeolites[a]

Sample	Al source	Si source
#6	$AlCl_3$	Na silicate
#7	$AlCl_3$	TEOS
#8	$Al(NO_3)_3$	TEOS
#9	$Al(NO_3)_3$	TEOS
#10	$Al(OH)_3$	TEOS
#11	$Al(OH)_3$	TEOS

[a] $T = 170\,^{\circ}C$, crystallization from 5 to 10 days. Template: tetrapropylammonium hydroxide.

$Al(NO_3)_3{\cdot}9H_2O$ (Fluka, 98%), $AlCl_3$ (Fluka, 99%) and $Al(OH)_3$ (Fluka, 65% Al_2O_3) were used as an aluminium source, and TEOS (tetraethoxyorthosilicate, Aldrich, 98%) and sodium silicate (Riedel–deHaën, 27% SiO_2, 10% NaOH) as a source of silica (see Table 2). TPA-OH (tetrapropylammonium hydroxide 20% solution in water, Fluka) served as a structure-directing agent. The syntheses were performed in autoclaves with agitation at a temperature of 170 °C under autogeneous pressure, as described elsewhere [10]. Zeolite products were washed by distilled water and dried at 80 °C. Calcination of the prepared samples was performed at 500 °C in a stream of air for 6 h.

Part of the calcined samples was ion-exchanged with 0.5 M NaCl at RT (100 ml of solution per 1 g of zeolite applied three times over 8 h). The Na-zeolites were then ion-exchanged with 0.05 M $Co(NO_3)_2$ (100 ml of solution per 1 g of zeolite applied three times over 8 h). These conditions of the Co ion exchange (specifically to the Na-form of the zeolite) guaranteed maximum exchange of the Co(II) ions (bound in dehydrated zeolites as bare cations), without exchanging the $[Co(II)–OH^-]^+$

monovalent species. The second part of the calcined samples was ion-exchanged with 0.5 M NH_4NO_3 at RT (100 ml of solution per 1 g of zeolite applied twice over 12 h). After each ion exchange procedure, the zeolites were carefully washed with distilled water and dried in the open air.

2.2. Analysis of the prepared ZSM-5 catalysts

The structure and crystallinity of the samples were checked by X-ray powder diffraction analysis on a Siemens 5005 diffractometer equipped with a graphite monochromator and scintillation counter, and using CuK_α radiation in Bragg–Bretano geometry. FTIR spectroscopy using the KBr technique was employed to estimate the crystallinity of the ZSM-5 zeolites. The spectra were recorded on a Nicolet Protégé 460 FTIR spectrometer equipped with an MCT/A detector. The size of the zeolite crystals was estimated from micrographs obtained with a scanning electron microscope Jeol (JSM-03).

^{29}Si and ^{27}Al MAS NMR experiments were carried out on a Bruker Avance 500 MHz (11.7 T) Wide Bore spectrometer using 4 mm o.d. ZrO_2 rotors with a rotation speed of 5 kHz for ^{29}Si MAS NMR and 12 kHz for ^{27}Al MAS NMR. A ^{29}Si MAS NMR high-power decoupling experiment with a $\pi/6$ (1.7 μs) excitation pulse and a relaxation delay of 30 s was employed to collect a single-pulse spectrum. The pulse sequence with 50% ramp CP pulse, contact time of 2000 μs, high-power decoupling and relaxation delay of 5 s was employed for the cross-polarization experiment. High-power decoupling pulse sequences with $\pi/12$ (0.7 μs) excitation pulses were employed to allow quantitative evolution of the ^{27}Al MAS NMR spectra. The chemical shifts were referenced to an aqueous solution of $Al(NO_3)_3$ for the ^{27}Al NMR spectra and to M8Q8 for the ^{29}Si NMR spectra.

The UV–vis spectra of the Co(II) ions were recorded on a Perkin–Elmer Lambda 19 UV–vis–NIR spectrometer equipped with a $BaSO_4$ integrating sphere. For the quantitative analysis, the spectra of the d–d transitions of bare Co(II) ions were deconvoluted to Gaussian bands and the absorption coefficients for the α-, β- and γ-types of Co(II) ions were used to determine the concentrations of the individual Co(II) ions. Details of the analysis are described elsewhere [15].

The concentrations of single and close aluminium atoms were determined from the bulk chemical composition of the CoNa-ZSM-5 samples.

$$[\text{single Al}] = [\text{Al}_{\text{total}}] - 2 \times [\text{Co}_{\text{max}}]$$

$$[\text{close Al}] = 2 \times [\text{Co}_{\text{max}}]$$

where [single Al] and [close Al] represent the concentrations of single and close aluminium atoms, respectively, $[\text{Al}_{\text{total}}]$ is the total concentration of aluminium and $[\text{Co}_{\text{max}}]$ is the concentration of cobalt in CoNa-ZSM-5 containing a maximum degree of the exchange of bare Co(II) ions. To complete the information on the location of the close Al atoms (for samples containing relatively high concentrations of close Al atoms), the concentration of close Al atoms in one six-membered ring [Al–O–(Si–O)$_2$–Al] was determined from quantitative analysis of the diffuse reflectance UV–vis spectra of CoNa-ZSM-5. Prior the spectral measurements, the samples were dehydrated at 100 °C for 30 min and 500 °C for 3 h under a vacuum. The concentration of close Al atoms in different framework rings, [Al–O–(Si–O)$_{n\geqslant 2}$–Al], was calculated as the difference between the total concentration of close Al atoms (obtained from chemical analysis of Co(II) ions) and the concentration of close Al atoms located in one six-membered ring (obtained from quantitative analysis of the d–d vis spectra of dehydrated CoNa-ZSM-5). It should be noted that evaluation of the effect of the concentration of close Al atoms and single Al atoms in the H-ZSM-5 was based on data obtained from chemical analysis of the Co(II) ions in zeolites.

The concentration of acidic Brønsted and Lewis sites in H-ZSM-5 was determined by adsorption of d_3-acetonitrile on zeolite samples evacuated at 500 °C, and quantitative analysis of the IR bands of C≡N vibrations. Adsorption of d_3-acetonitrile (13 mbar) was carried out at 298 K with subsequent evacuation for 15 min at the same temperature prior to FTIR spectral measurements. The IR spectra were recorded on a Nicolet Magna 550 FTIR spectrometer operating at 2 cm^{-1} resolution by collecting 200 scans for a single spectrum. The extinction coefficients for C≡N vibrations associated with Brønsted and Lewis sites were taken from Ref. [25].

Information on the acid strengths of the OH groups was based on the IR spectra of hydrogen adsorbed at 20 K at a pressure of 50 mbar, yielding the position of the H–H vibration and the shift of the bridging OH groups. An FTIR spectrometer (EQUINOX 55, Bruker) operating at 1 cm^{-1} resolution and collecting 256 scans for a single spectrum was employed. A cryogenic apparatus was used for in situ activation of the zeolite sample under high vacuum ($p < 10^{-5}$ mbar), and subsequent dosage of hydrogen under controlled temperature and pressure; the details of procedure were given elsewhere [26].

2.3. Catalytic experiments

Powder catalysts were pelletized and sieved to a particle size of 0.5 mm. Calcination of the catalysts was performed under an oxygen stream at 500 °C for 2 h. The catalytic test was carried out in a fixed-bed flow-through reactor at 500 °C, atmospheric pressure and GHSV of 15 or 30 h^{-1}. The amount of the catalyst was typically 300 mg. The feed contained 50% of 1-butene and 50% of N_2. The reaction products were analyzed by an on-line-connected gas chromatograph (Finnigan 9001) equipped with an Al_2O_3/KCl capillary column.

3. Results and discussion

3.1. Structure of ZSM-5 zeolites

We had in mind that a high number of structural and textural parameters of zeolites might be reflected in their activity. Therefore, for analyzing the effect of Al distribution in the framework on the zeolite activity, we attempted to select samples with well-developed structure, similar compositions and close crystal size dimensions. SEM micrographs, XRD diffraction patterns, ^{27}Al

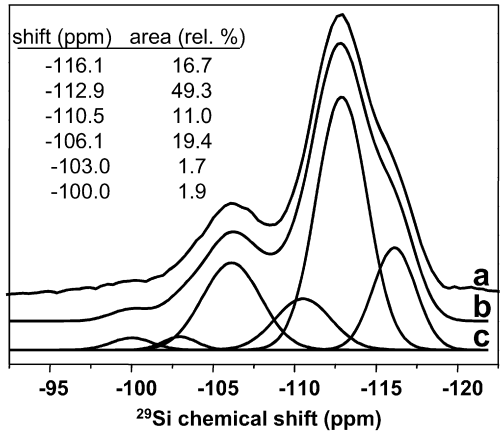

Fig. 1. ^{29}Si MAS NMR spectrum of ZSM-5 sample #6 (a) experimental, (b) simulated spectrum and (c) Gaussian bands corresponding to the individual resonances.

MAS NMR and ^{29}Si MAS NMR spectra of ZSM-5 zeolites are available in the Supplementary material.

SEM micrographs of the synthesized ZSM-5 samples served for estimation of the average crystal size of the synthesized and commercial samples (given in Table 1). Samples #7–11, prepared by using TEOS as a silicon source, exhibited a crystal size in the range from 0.3–0.6 μm, and sample #6, synthesized by using sodium silicate, consists of crystals of about 5 μm in size. Diffraction patterns and FTIR spectra of skeletal vibrations of the as-synthesised and calcined ZSM-5 zeolites indicated high crystallinity of the prepared samples.

The strong band with a chemical shift of about 55 ppm in the ^{27}Al MAS NMR spectra of hydrated Na-ZSM-5 zeolites indicated the presence of more than 97% Al in the framework in tetrahedral coordination for samples #2–11; the very low intensity of the peak at 0 ppm indicated less than 3% rel. of Al in octahedral coordination in the extra-framework positions. Only sample #1 contained approx. 10% of Al atoms in octahedral coordination at extra-framework sites.

^{29}Si MAS NMR spectrum of the hydrated Na-ZSM-5 (sample #6) and its simulation is shown in Fig. 1. It is similar to those reported previously for ZSM-5 zeolites [14]. The spectra of the other samples are given in the Supplementary material. The resonances at −112.9 and −116.1 ppm were assigned to the Si (4Si,0Al) sites. The bands at −103.0, −106.1 and −110.5 ppm correspond to Si (3Si,1Al) sites, i.e. Si atoms with one neighbouring Al atom. The resonance at −100.0 ppm can be attributed to Si (3Si,1OH) sites, as supported by the cross-polarization experiment (not shown in the figure). Resonances with chemical shifts below −100 ppm representing Si (2Si,2Al) sites with two Al neighbours were not observed. The spectra of the other samples were similar and also did not contain any bands corresponding to Si (2Si,2Al) atoms. This finding indicates that [Al–O–Si–O–Al] sequences are not present in the investigated samples. Therefore, the closest Al atoms are represented by the [Al–O–(Si–O)$_2$–Al] sequences.

The silicon to framework aluminium ratio (see Table 1) of the samples (Si/Al$_{FR}$) was estimated using the Si/Al$_{FR}$ = $I/0.25I_1$ equation, where I denotes the total intensity of the

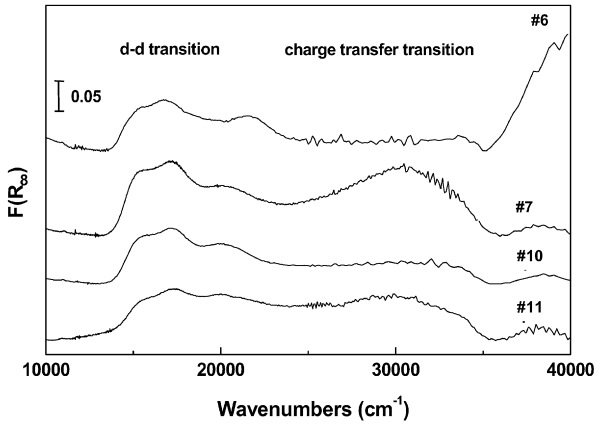

(A)

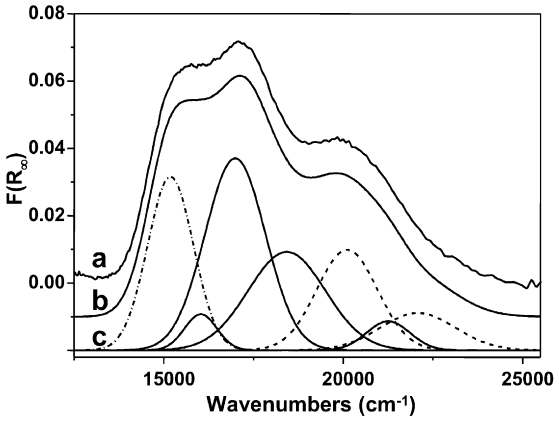

(B)

Fig. 2. (A) UV–vis spectra of the synthesized and calcined Co-ZSM-5 with maximum Co(II) loading; the spectra of Co-ZSM-5 with low Co(II) exchange capacity are not shown. (B) Simulation of vis spectra of calcined and dehydrated Co-ZSM-5 (sample #10). (a) Experimental data, (b) spectrum simulation and (c) individual Gaussian bands corresponding to the bare Co(II) ion in the α- (···), β- (—) and γ-site (- - -).

^{29}Si NMR signal in the single pulse experiment and I_1 denotes the intensity of the NMR line corresponding to the Si (3Si,1Al) atoms [27]. These values of Si/Al$_{FR}$ of samples #2–11 correspond well to the Si/Al values obtained from the chemical analysis. This confirms the assignment of the individual resonances to the individual types of Si sites and also indicates that the concentration of the extra-framework Al atoms is negligible. The Si/Al$_{FR}$ = 17 value of sample #1 is slightly higher than the value obtained from chemical analysis (Si/Al = 15.8). This indicates that approx. 10% of Al in sample #1 corresponds to extra-framework Al species. Therefore, the concentration of extra-framework Al estimated by ^{29}Si MAS NMR agrees well with the concentration estimated using ^{27}Al MAS NMR.

The UV–vis spectra of dehydrated Co-ZSM-5 are depicted in Fig. 2A. The spectra of Co-ZSM-5 exhibited a broad band ranging from 14 000 to 22 000 cm^{-1}, corresponding to the d–d transitions of bare Co(II) cations in the α-, β- and γ-types of cationic sites (for details, see Ref. [15]). The deconvolution of the broad d–d band of the Co(II) ions in Co-ZSM-5 zeolite originated from sample #10 is for illustration given in Fig. 2B. The positions of the individual bands of Co components were

Table 3
Al–O–(Si–O)$_n$–Al sequences in the framework of ZSM-5 zeolite

	Sequence	Position of the sequence	Identification
Close aluminium	Al–O–(Si–O)–Al	Not found	^{29}Si MAS NMR
Close aluminium	Al–O–(Si–O)$_2$–Al	In one six-member ring	The charge is balanced by exchanged [Co(H$_2$O)$_6$](II) ions in a hydrated zeolite or by bare Co(II) in a dehydrated zeolite; d–d transitions of [Co(H$_2$O)$_6$](II) or Co(II)
Close aluminium	Al–O–(Si–O)$_{n\geqslant 2}$–Al	In different neighbouring rings	The charge is balanced by [Co(H$_2$O)$_6$](II) ions in a hydrated zeolite and by Co–oxo species in a dehydrated zeolite; d–d electron transitions of [Co(H$_2$O)$_6$](II) and charge transfer transition of Co–oxo species
Single aluminium	Al–O–(Si–O)$_{n>2}$–Al	–	The charge cannot be balanced by exchanged [Co(H$_2$O)$_6$](II) ions or bare Co(II) ions

taken from Ref. [15] on the basis of the spectral analysis of Co-ZSM-5 containing a predominant amount of one Co component. The extinction coefficients for the α-, β- and γ-type Co(II) ions in CoNa-ZSM-5 were taken from Ref. [15]. As the studied samples do not exhibit [Al–O–Si–O–Al] sequences, the bare Co(II) ions in dehydrated zeolites should be compensated by a negative framework charge given by the [Al–O–(Si–O)$_2$–Al] sequence in a cationic site, and should be coordinated to a single six-membered ring. Thus, the intensity of the d–d bands of bare Co(II) ions represents a measure of the concentrations of close Al atoms in one six-membered ring ([Al–O–(Si–O)$_2$–Al] sequences), see Table 1.

In some Co-ZSM-5 samples, an intense band at about 30 000 cm^{-1} was found in the UV–vis spectra. This corresponds to the charge-transfer absorption of some bridging Co–O$_x$–Co species (see Fig. 2A). The Co–O$_x$–Co species might be formed after dehydration of Co-ZSM-5 from the [Co(H$_2$O)$_6$](II) complexes balanced by close Al atoms in different rings and separated by two or more silicon-oxygen groups. Thus, the intensity of the band around 30 000 cm^{-1} indirectly reflects the concentration of close Al atoms located in different rings of the framework. This approach to analysis of the Al distribution through the zeolite framework is described in detail in Refs. [8,9]. It should be noted that the absorption coefficient of the charge transfer band of Co(II) ions in zeolites is approximately 50 times higher than that of the d–d transitions. Therefore, the relatively intense band at 30 000 cm^{-1} observed for samples #7 and #11 reflects a rather low concentration of close Al atoms in different rings [Al–O–(Si–O)$_{n\geqslant 2}$–Al], equal to 0.018 and 0.019 mmol/g compared to those in one ring (cf. Ref. [28]). For samples #6, #8 and #9, the CT band was of such low intensity that it could not be quantitatively analyzed. The predominant concentrations of close Al atoms located in one ring (cationic sites) among those in different rings for all the samples indicate that large numbers of close Al atoms are represented by "Al pairs" (Al–O–(Si–O)$_2$–Al) sequences in cationic sites.

It is concluded that the Si–Al sequences which charge-balance the Co(II) ions in hydrated zeolites, i.e. both [Al–O–(Si–O)$_2$–Al] sequences, in one six-membered ring and [Al–O–(Si–O)$_{n\geqslant 2}$–Al] sequences in different rings, represent close Al atoms providing close protonic sites (see Table 3 for description and the method of identification). The single aluminium atoms are located in the [Al–O–(Si–O)$_{n>2}$–Al] sequences. Thus, only one Al atom is present in the six- or five-membered rings, bearing one negative charge and thus it is able to balance only a monovalent cation or monovalent complex.

The relative concentrations of close Al atoms and of single Al atoms determined from the ion-exchange capacity for [Co(H$_2$O)$_6$](II) ions are listed in Table 1. We prepared and selected four pairs of samples, i.e. #1 and #6, #8 and #7, #9 and #10, and #2 and #11 with close Si/Al ratios of about 14, 28, 38 and 43, respectively, but with quite different distribution of aluminium, to analyze its effect on the zeolite activity in butene transformation.

3.2. Acid sites and their acid strength

The pair of samples #7 and #8, exhibiting similar Si/Al ratios of ∼28, but substantially different concentrations of close and thus also single Al atoms, was chosen for analysis of the acid strength of the protonic sites. Typical IR bands characteristic for bridging OH groups of H-ZSM-5 at 3612 cm^{-1} and a band at 3745 cm^{-1} reflecting the presence of terminal Si–OH groups were found at RT (not shown in the figure). No absorption was observed in the region of the Al–OH groups at approx. 3650 cm^{-1}. Adsorption of d_3-acetonitrile resulted in the complete disappearance of the band at 3612 cm^{-1}, while the band of the Si–OH groups was much less affected, and in the appearance of the bands at 2360–2220 cm^{-1} (Fig. 3). The deconvolution procedure yielded the bands at 2325, 2297, 2280 and 2252 cm^{-1}. The bands at 2325 and 2297 cm^{-1} correspond to the stretching mode of ν(C≡N) of d_3-acetonitrile adsorbed on Lewis and Brønsted sites, respectively [25]. The bands at 2280 and 2252 cm^{-1} reflect the interaction of C≡N groups with terminal Si–OH groups, and the physically sorbed acetonitrile, respectively. Quantitative analysis of the acid sites using the integral intensities of the IR bands and the extinction coefficients for the C≡N group interacting with the Brønsted and Lewis sites [25] indicated a highly predominant concentration of Brønsted sites and low concentration of Lewis sites in both samples #7 and #8 (Table 4). In all cases, samples #1, #2 and #6–11 exhibited less than 10% of Lewis sites, as measured by the IR spectra of adsorbed d_3-acetonitrile.

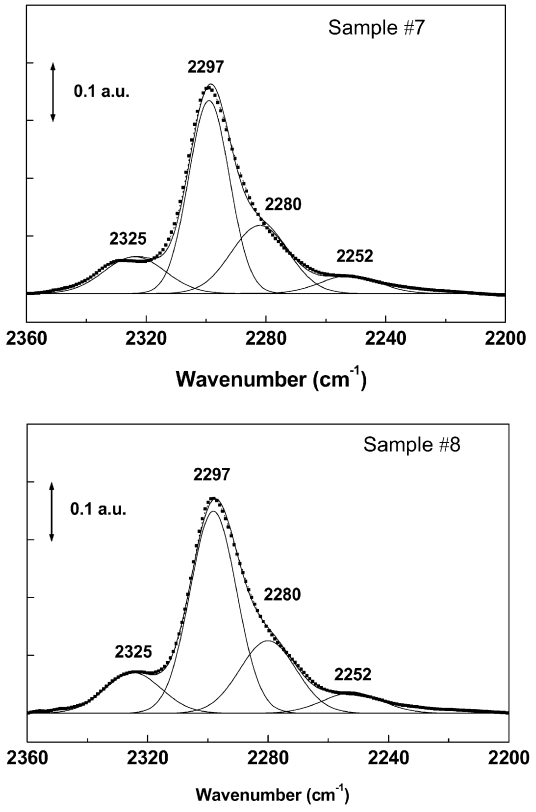

Fig. 3. FTIR spectra after adsorption of d_3-acetonitrile (13 mbar) at RT and evacuation at RT on ZSM-5 zeolites (sample #7 and sample #8).

Table 4
Concentration of aluminium, Brønsted and Lewis sites in ZSM-5 (samples #7 and #8)

Sample	Si/Al	Aluminium[a] (mmol/g)	Brønsted site[b] (mmol/g)	Lewis site[b] (mmol/g)
#7	26.8	0.59	0.45	0.06
#8	28.6	0.56	0.43	0.05

[a] Chemical analysis.
[b] FTIR using adsorption of d_3-acetonitrile.

The perturbation of a hydrogen molecule adsorbed on the surface results in a polarization effect leading to the appearance of an induced dipole moment and hence to the IR activity [29,30]. The induced dipole moment and thus the frequency of the IR band might be sensitive to surface heterogeneity [29, 30]. Makarova et al. [31] and Zecchina et al. [32] considered perturbation of adsorbed hydrogen as a convenient probe for estimation of the acid strength of the Brønsted sites of zeolites with various structures, by measuring the shift in the H–H and OH modes. Sigl et al. [29] have shown that the IR frequency shift of H–H is sensitive to the acid strength of ZSM-5 zeolites with Al, Ga and Fe substituted frameworks.

The IR spectrum of calcined and evacuated H-ZSM-5 zeolites (samples #7 and #8) monitored at 20 K exhibited typical characteristic bands for bridging OH groups and terminal Si-OH groups. The bands were shifted from 3612 to 3623 cm^{-1} and from 3745 to 3750 cm^{-1}, respectively, due to the low temperature effect. After adsorption of hydrogen at 20 K, the band

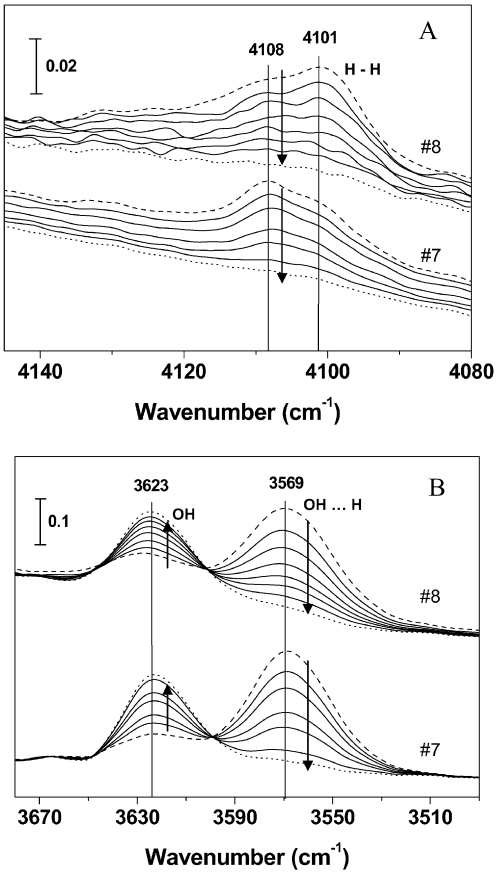

Fig. 4. FTIR spectra of adsorbed hydrogen ($p = 50$ mbar) on H-ZSM-5 zeolites (samples #7 and #8 outgassed at 748 K) at 20 K in the region of (A) ν(H–H) mode and (B) ν(O–H) mode bridging OH groups; (- - -) after hydrogen adsorption and evacuation at 20 K for 40 min and (···) for 140 min at 20 K (complete hydrogen desorption).

of bridging OH groups at 3623 cm^{-1} was shifted to 3569 cm^{-1} and new bands at 4101 ($\Delta\nu$H–H $= -60$ cm^{-1}) and 4108 cm^{-1} ($\Delta\nu$H–H $= -55$ cm^{-1}) appeared due to the ν(H–H) mode of the adsorbed hydrogen (cf. Refs. [31,33]). Simultaneously, low-intensity absorption appeared in the 4020–4150 cm^{-1} region due to hydrogen interacting with silanols and also corresponding to physisorbed hydrogen. After evacuation of the samples, the latter bands disappeared as did the frequency shift of silanol groups (not shown in the figure). The evolution of the spectra in the region of the vibration of the adsorbed H_2 (ν(H–H) mode) and of the bridging OH groups (ν(O–H) mode) during evacuation is displayed in Figs. 4A and 4B, respectively. It is evident that the decrease in the intensities of the 4101 and 4108 cm^{-1} components during desorption of hydrogen is strictly related to the increase in the band at 3623 cm^{-1} of the unperturbed bridging OH groups, and to the decrease in the intensity at 3569 cm^{-1} of the stretching mode in the 1:1 (O–H)···H_2 complex [31,33]. Simultaneously, the very weak broad band at 4133 cm^{-1} ($\Delta\nu$H–H $= -28$ cm^{-1}) assigned to the ν(H–H) mode of adsorbed hydrogen on non-protonic less-polarizable surface sites substantially decreased. The positions of the absorption bands at 4101 and 4108 cm^{-1} due to the stretching vibrations of hydrogen on Brønsted sites are the same for both

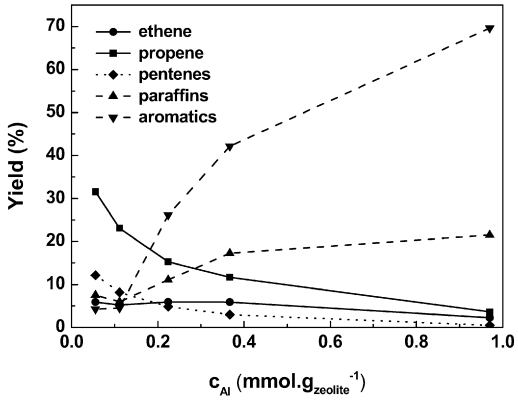

Fig. 5. Yield of ethene, propene, pentenes, aromatics and paraffins in cracking of 1-butene over H-ZSM-5 as a function of aluminium content. $T = 500\,^{\circ}\mathrm{C}$, GHSV $= 15\ \mathrm{h}^{-1}$; samples #1, #2, #3, #4 and #5.

samples, but the ratio of the intensity of the individual components differs. The splitting of the vibration of hydrogen adsorbed on a Brønsted site into two bands has not been explained yet. It has been proposed that the bands at 4101 and 4108 cm^{-1} can be assigned to ortho- and para-H_2, respectively, adsorbed on the same sites [34]. The same position of the peaks corresponding to the ν(H–H) mode of the adsorbed H_2 and the same shift of the OH groups ($\Delta\nu$O–H) due to the formation of the 1:1 (O–H)$\cdots H_2$ complex on samples #7 and #8 show that the acid strengths of their OH groups does not differ significantly.

Thus, the same strength of interaction of H_2 with acid OH groups in the (O–H)$\cdots H_2$ complex is obvious for both zeolite samples with different concentrations of close Al atoms. This finding indicates a similar strength of all the bridging OH groups. The different types of OH groups of H-ZSM-5, with respect to vibration of the OH groups, reported by Datka et al. [3], can therefore not be unambiguously connected with their different acid strengths. Calorimetric data for the adsorption of ammonia as well as the linear increase in the activity of H-ZSM-5 zeolites with increasing Al content in cracking of paraffins [2] are also strong arguments for the homogeneity of the OH groups with respect to their deprotonation. Nevertheless, for transformation of olefins where a mono- or bimolecular reaction pathway can be involved, the distribution of the Al atoms through the framework and thus of protonic sites might play a role.

3.3. Activity of H-ZSM-5 zeolites in cracking of 1-butene

Fig. 5 depicts the effect of the aluminium content in the framework of ZSM-5 zeolites on the yields of products in cracking of 1-butene. High yields of propene, ethene and pentenes are observed for very low concentrations of aluminium and thus of the protonic sites in ZSM-5 zeolites. It should be mentioned that the yields of 40% of the sum of $C_2^{=} + C_3^{=}$ are promising for technical applications and that propene is preferred product from a technical viewpoint. The higher yields of $C_3^{=}$ and $C_5^{=}$ compared to ethene indicate dimerization of butene to $C_8^{=}$ olefins and their cracking mainly to $C_3^{=}$ and $C_5^{=}$ olefins. Thus, the reaction pathway of butenes to propene proceeds via their dimerization with subsequent cracking. The lower yield of $C_5^{=}$ compared to that of $C_3^{=}$ indicates easier cracking and oligomerization of the former olefin. With an increasing aluminium content, the yields of aromatics and paraffins increase and the yields of $C_3^{=}$ and $C_5^{=}$ decrease, while the yield of ethene does not change substantially. This indicates increasing participation of the oligomerization and hydrogen transfer reactions with higher concentration of acid sites, yielding aromatics and paraffins.

In the mechanistic considerations of the acid-catalyzed cracking of olefins, the group of Haag at Mobil Oil Corp. showed that the rate of cracking of olefins increases dramatically with the carbon number [18]. While the rate of cracking for C_5–C_8 paraffins is increased only approx. 10 times, it is 500 times higher for C_5–C_8 olefins. They also suggested that the olefin cracking is connected with the monomolecular pathway, which can be preferred for short contact times.

3.4. The effect of aluminium distribution on the product yields in cracking of 1-butene

As the product composition depends strongly on the concentration of protonic sites and thus aluminium content in the zeolite framework, we attempted to compare samples exhibiting similar framework compositions. Four pairs of samples, #1 and #6, #7 and #8, #9 and #10, and #2 and #11 with similar Si/Al ratios of about 14, 28, 38 and 43, respectively, but different distributions of framework aluminiums, were tested in 1-butene transformation. The results for the samples including both commercial samples and those synthesized in the laboratory are given in Figs. 6A–6D. It can be seen for all the samples that a higher relative concentration of single Al atoms in samples possessing similar concentration of protonic sites results in higher yields of propene, ethene and pentenes and lower yields of aromatics. On contrary, the higher relative concentrations of close Al atoms in the zeolites favour the formation of aromatics. Thus, the results indicate that the close aluminium atoms enhance hydrogen transfer reactions leading to aromatics at the expense of cracking reactions.

It should be mentioned that we did not observe the same trend for the yields of paraffins, although they might follow the pattern of aromatics. As our samples did not contain a metallic component, it can be expected that part of transferred hydrogen was released into the gas phase without hydrogenation of olefins (hydrogen was not analyzed in the products). Samples #1, #2, #7–#11, compared with respect to their Al distribution and activity, exhibited small crystals below 1 μm for which diffusion limitations could be neglected. This allowed the observation of the effect of the aluminium distribution on the yield of the individual products. However, sample #6 with crystal size of 5 μm exhibited slightly lower conversion and faster deactivation compared to other samples with small crystals, and thus also the yield of the products might be affected by the product transport in the larger crystal size. Thus, for this sample, in addition to the effect of distribution of Al in the framework, the yield of individual products could be affected by intra-crystalline diffusion.

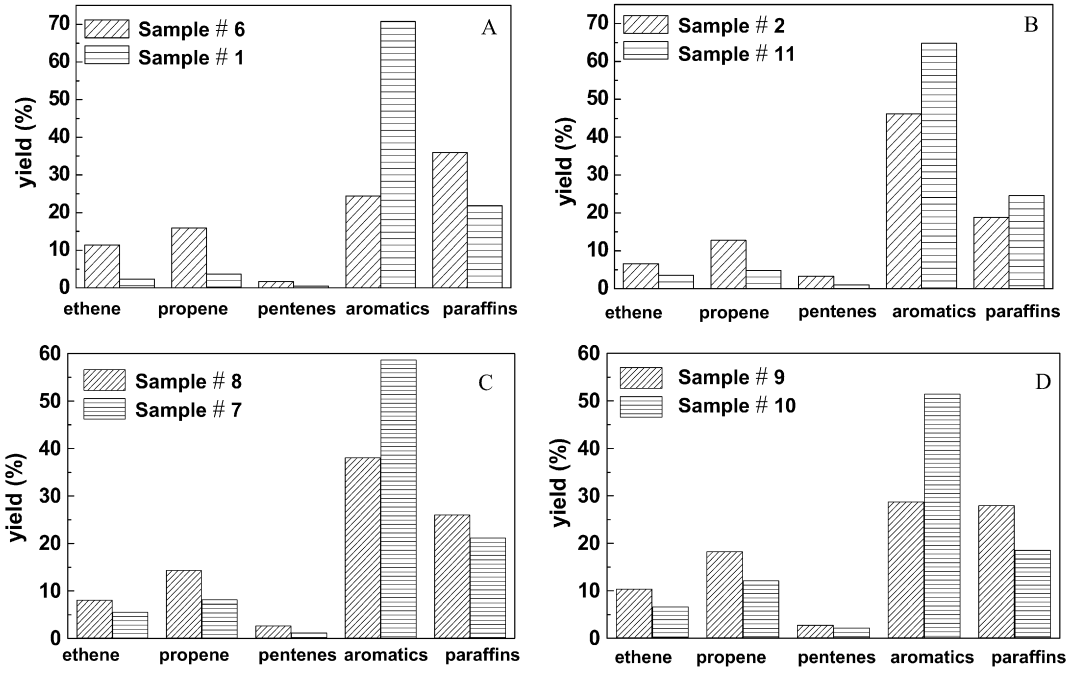

Fig. 6. Cracking of 1-butene over H-ZSM-5, effect of Al distribution on the yields of products. Reaction conditions: $T = 500\,^{\circ}\mathrm{C}$, TOS = 20 min, GHSV = 15 or 30 h^{-1}. (A) sample #6 (16% close Al, Si/Al = 12.6), sample #1 (32% close Al, Si/Al = 15.8); (B) sample #2 (15% close Al, Si/Al = 43.6), sample #11 (42% close Al, Si/Al = 43.3); (C) sample #8 (6% close Al, Si/Al = 28.6), sample #7 (36% close Al, Si/Al = 26.8); (D) sample #9 (10% close Al, Si/Al = 37.4), sample #10 (44% close Al, Si/Al = 37.9).

4. Conclusions

The present investigation of the acid-catalyzed transformation of 1-butene over synthesized and commercial H-ZSM-5 zeolites differing in the Al distribution in the framework showed that the local aluminium distribution in the framework of H-ZSM-5 affects the product composition during cracking of olefins. We exploit the finding [9,10] that the local Al distribution in the framework of ZSM-5 can be controlled by the conditions of zeolite synthesis. The concentration of relatively "close" and "single" (far distant) protons, controlled by the location of the Al in the framework in ZSM-5 was estimated from the Co(II) ion-exchange capacity in hydrated zeolites, and quantitative analysis of characteristic d–d and charge-transfer transitions in the UV–vis spectra of Co(II) ions in dehydrated zeolites. As the ^{29}Si MAS NMR spectra showed absence of Si (2Si2Al) sites (Al–O–Si–O–Al sequences), only Al–O–(Si–O)$_{n=2}$–Al sequences balance the Co(II) ions, while far distant Al atoms are represented by Al–O–(Si–O)$_{n>2}$–Al sequences.

It has been shown that, in addition to the overall concentration of protonic sites, the particle size of zeolite crystals and the contact time employed, the selectivity of the catalytic process is significantly affected by the local distribution of protonic sites in the ZSM-5 zeolite governed by the location of aluminium in the framework. Distant single Al atoms and thus single protons support cracking of butenes and octenes (formed by dimerization). Relatively "close" Al atoms, providing "close" protonic sites, enhance oligomerizarion and hydrogen transfer reactions leading to aromatics. As the perturbation of the H–H mode of hydrogen adsorbed on Brønsted sites did not reveal a significant difference in the acid strength of such located protonic sites, this result supports previous conclusions in the literature on the similar acid strength of Brønsted sites in ZSM-5 zeolites. Therefore, the obtained results on the transformation of 1-butene over H-ZSM-5 indicate that the local distribution of Al in the framework has a significant effect on the reaction pathway of olefin transformation.

For many acid-catalyzed reactions, e.g., paraffin cracking, benzene alkylation with olefins [2,35], it has been shown that the activity of H-ZSM-5 zeolites is proportional to the concentration of aluminium in the framework. However, substantially different yields of olefins and aromatics in the reaction of 1-butene cracking over H-ZSM-5 zeolites with similar Si/Al framework ratio and crystal size, but different relative concentrations of "close" and "single" framework Al atoms, leads us to the conclusion that the distribution of Al in the framework affects the product composition in the processes involving mono- and bi-molecular and hydrogen transfer reactions. This finding, together with the successful attempt to change the Al distribution in the framework of ZSM-5 zeolites through the conditions of their synthesis [9,10], therefore opens a new perspective for tailoring the selectivity of zeolite-based catalysts for acid-catalyzed reactions.

Acknowledgments

This study was performed within the EU Network of Excellence IDECAT #NMP 3-CT-2005-011730 and supported by the project #IAA4040308 of the Grant Agency of the Academy of Sciences and project #KAN100400702 of the Academy of Sciences of the Czech Republic, and the project #203/03/H140 of the Science Foundation of the Czech Republic.

Supplementary material

The on-line version of this article contains supplementary material containing SEM micrographs, XRD, ^{27}Al and ^{29}Si MAS NMR spectra of ZSM-5 zeolites.

Please visit DOI: 10.1016/j.jcat.2007.12.005.

References

[1] G.T. Kokotailo, S.L. Lawton, D.H. Olson, W.M. Meier, Nature 272 (1978) 437.
[2] D.H. Olson, W.O. Haag, ACS Symp. Ser. 248 (1984) 275.
[3] J. Datka, B. Gil, P. Baran, Microporous Mesoporous Mater. 58 (2003) 291.
[4] C.D. Chang, Catal. Rev. 26 (1984) 323.
[5] S.M. Csicsery, Zeolites 4 (1984) 202.
[6] O. Bortnovský, P. Sazama, B. Wichterlová, Appl. Catal. A 287 (2005) 203.
[7] X.X. Zhu, Sh. Liu, Y.Q. Song, L.Y. Xu, Appl. Catal. A 288 (2005) 134.
[8] J. Dědeček, D. Kaucký, B. Wichterlová, Chem. Commun. (2001) 970.
[9] J. Dědeček, D. Kaucký, B. Wichterlová, O. Gonsiorová, Phys. Chem. Chem. Phys. 4 (2002) 5406.
[10] V. Gábová, J. Dědeček, J. Čejka, Chem. Commun. (2003) 1196.
[11] P. Sarv, C. Fernandéz, J.P. Amoureux, K. Keskinen, J. Phys. Chem. 100 (1996) 19223.
[12] P. Sarv, B. Wichterlová, J. Čejka, J. Phys. Chem. B 102 (1998) 1372.
[13] S. Sklenák, J. Dědeček, Ch. Li, B. Wichterlová, V. Gábová, M. Sierka, J. Sauer, Angew. Chem. Int. Ed. 46 (2007) 7286.
[14] C.A. Fyfe, C.G. Gobbi, G.J.J. Kennedy, J. Phys. Chem. 88 (1984) 3248.
[15] J. Dědeček, D. Kaucký, B. Wichterlová, Microporous Mesoporous Mater. 35–36 (2000) 483.
[16] J. Weitkamp, P.A. Jacobs, J.A. Martens, Appl. Catal. A 8 (1983) 123.
[17] J.A. Martens, P.A. Jacobs, in: J.B. Moffat (Ed.), Theoretical Aspects of Heterogeneous Catalysis, Van Nostrand Reinhold, New York, 1990.
[18] J.S. Buchanan, J.G. Santiesteban, W.O. Haag, J. Catal. 158 (1996) 279.
[19] European Communication, October 1999.
[20] J.-P. Dath, L. Delorme, Eur. Patent 0 921 181 (1999) to Fina Research.
[21] F.-W. Moeller, P. Kleniv, US Patent 5 981 819 (1999) to Metallgesellschaft Aktiengesellschaft.
[22] D.L. Johnson, N. Khushrav, US Patent 6 222 087 (2001) to Mobil Oil Corporation.
[23] P.K. Ladwig, J.E. Adélin, US Patent 6 313 366 (2001) to ExxonMobile Chemical Patents, Inc.
[24] O. Bortnovský, O. Gonsiorová, J. Kolena, G. Stavová, A. Soukup, B. Wichterlová, Z. Sobalík, CZ Patent 20040494 (2005) to Výzkumný ústav anorganické chemie, a. s.
[25] B. Wichterlová, Z. Tvarůžková, Z. Sobalík, P. Sarv, Microporous Mesoporous Mater. 24 (1998) 223.
[26] G. Spoto, E.N. Gribov, G. Ricchiardi, A. Damin, D. Scarano, S. Bordiga, C. Lamberti, A. Zecchina, Prog. Surf. Sci. 76 (2004) 71.
[27] G. Engelhardt, U. Lohse, E. Lippmaa, M. Tarmak, M. Magi, Z. Anorg. Allg. Chem. 482 (1981) 49.
[28] J. Dědeček, L. Čapek, D. Kaucký, Z. Sobalík, B. Wichterlová, J. Catal. 211 (2002) 198.
[29] M. Sigl, S. Ernst, J. Weitkamp, H. Knözinger, Catal. Lett. 45 (1997) 27.
[30] E.N. Gribov, D. Cocina, G. Spoto, S. Bordiga, G. Ricchiardi, A. Zecchina, Phys. Chem. Chem. Phys. 8 (2006) 1186.
[31] M.A. Makarova, V.L. Zholobenko, K.M. Al-Ghefaili, N.E. Thompson, J. Dewing, J. Dwyer, J. Chem. Soc. Faraday Trans. 90 (1994) 1047.
[32] A. Zecchina, G. Spoto, S. Bordiga, Phys. Chem. Chem. Phys. 7 (2005) 1627.
[33] M. Makarova, F.A. Ojo, K. Karim, M. Hunger, J. Dwyer, J. Phys. Chem. 98 (1994) 3619.
[34] I.N. Senchenya, V.B. Kazansky, Kinet. Catal. 35 (1994) 80.
[35] J. Čejka, B. Wichterlová, Catal. Rev. 44 (2002) 375.